

University of Nebraska - Lincoln

DigitalCommons@University of Nebraska - Lincoln

Faculty Publications from the Department of
Electrical and Computer Engineering

Electrical & Computer Engineering, Department of

11-1-1996

Oxygen plasma asher contamination: An analysis of sources and remedies

R. A. Synowicki

University of Nebraska - Lincoln

Jeffrey S. Hale

University of Nebraska - Lincoln

William A. McGahan

University of Nebraska - Lincoln

Natale J. Ianno

University of Nebraska - Lincoln, nianno1@unl.edu

John A. Woollam

University of Nebraska-Lincoln, jwoollam1@unl.edu

Follow this and additional works at: <http://digitalcommons.unl.edu/electricalengineeringfacpub>



Part of the [Electrical and Computer Engineering Commons](#)

Synowicki, R. A.; Hale, Jeffrey S.; McGahan, William A.; Ianno, Natale J.; and Woollam, John A., "Oxygen plasma asher contamination: An analysis of sources and remedies" (1996). *Faculty Publications from the Department of Electrical and Computer Engineering*. 72.

<http://digitalcommons.unl.edu/electricalengineeringfacpub/72>

This Article is brought to you for free and open access by the Electrical & Computer Engineering, Department of at DigitalCommons@University of Nebraska - Lincoln. It has been accepted for inclusion in Faculty Publications from the Department of Electrical and Computer Engineering by an authorized administrator of DigitalCommons@University of Nebraska - Lincoln.

Oxygen plasma asher contamination: An analysis of sources and remedies

R. A. Synowicki, Jeffrey S. Hale, William A. McGahan, N. J. Ianno,
and John A. Woollam^{a)}

*Center for Microelectronic and Optical Materials Research and Department of Electrical Engineering,
University of Nebraska-Lincoln, Lincoln, Nebraska 68588-0511*

(Received 20 January 1996; accepted 23 August 1996)

The low Earth orbit (LEO) environment is commonly simulated using oxygen plasma ashers to determine the effects of LEO on spacecraft materials. However, plasma ashers can also contaminate samples during plasma exposure, making them less than ideal for space simulation. This study results from attempts to minimize or eliminate contamination. Optical methods of variable angle spectroscopic ellipsometry and reflectance spectrophotometry were used to quantify contaminant stoichiometry and deposition rate. Auger electron spectroscopy identified deposited contaminants and their surface coverage. Contamination results from etching of the rubber chamber seals by the plasma. The deposited contaminant was nearly indistinguishable from fully stoichiometric SiO₂. Contaminant deposition rates up to 0.27 nm/min have been observed, and these layers effectively passivate the surface by depositing an overcoat of SiO_x. Placing metal into the path of the plasma before it can reach the chamber seals greatly reduces contamination. A newly designed chamber confines the plasma to a small volume away from the chamber seals. For fluences as high as 3.5×10^{22} atoms/cm², equivalent to 7.5 years of space exposure for the International Space Station, the redesigned asher showed less than one monolayer of deposited contaminant. © 1996 American Vacuum Society.

I. INTRODUCTION

The development of durable spacecraft coatings and structural materials requires accurate simulation of the low Earth orbit (LEO) environment.^{1,2} An oxygen plasma generated inside an evacuated chamber is commonly used for this purpose. This method is known as "ashing" and is very popular due to its minimal cost, simplicity, and high flux of reactive species. However, low kinetic energy, lack of directionality in the reactive species, and contamination are drawbacks to this simulation method. Commercial ashing systems have been designed for short exposures to low fluence, as used in the semiconductor industry. However, for accurate space simulation, long ashings to high fluences are needed to simulate long-term LEO exposure. Deposition of contaminant overlayers is a severe problem in simulation measurements since the layers serve to protect the surface of interest from the reactive species. Minimizing contaminant deposition thus becomes a prerequisite for establishing the effectiveness of plasma ashers for LEO simulation. Space simulation researchers have been aware of contamination for some time, but a quantitative study of its effects has not yet been published.

Contaminants and their deposition rate were identified in order to determine their cause and minimize their effects. Samples of metal thin films were exposed in a commercially available plasma reactor (Plasma Prep II, manufactured by Structure Probe Incorporated). Comparison is made with results from a custom built system designed for minimum deposited contaminant in exposures to high fluence.

II. EXPERIMENT

Aluminum and gold were chosen as the metal films for study, and were either sputtered to a thickness of 100 nm, or electron-beam evaporated to a thickness of 70 nm. All gold films were sputtered to a thickness of 100 nm. The substrates were fused silica and wafers of silicon or gallium arsenide.

The Plasma Prep II chamber configuration is shown in Fig. 1, and consists of two Pyrex chambers sealed with a buna-n (natural rubber) gasket. Note that upon close examination, Fig. 1 shows a small ring-shaped area of exposed rubber gasket between the two chamber halves. The chamber base pressure is nominally 50 mT, and then is backfilled with oxygen gas to approximately 100 mT. This can be considered a "dirty" vacuum since the gas composition is 50% air and 50% oxygen. The nitrogen component of the plasma should not significantly alter the reactivity of the plasma or the reaction end products of the materials since the oxygen present is much more reactive than the nitrogen. Therefore, extreme cleanliness with respect to nitrogen is not required of the vacuum. Application of 100 W rf power at 13.56 MHz to electrodes surrounding the chamber excites the plasma. Mass loss of kapton polyimide is used to calibrate exposure in the asher against that received in LEO. Kapton mass loss has been calibrated against ashing exposure (fluence) in both laboratory and orbital experiments, and thus mass loss of kapton is often used to calibrate effective space exposure in chambers used for space simulation.³

The thickness and composition of the contaminant films were determined by reflectance spectrophotometry in the ultraviolet (UV), visible, and near infrared, where changes in specular reflectance as a function of asher exposure were measured from 250 to 2300 nm. Interference effects are seen

^{a)}Electronic mail: jwoollam@unl.edu

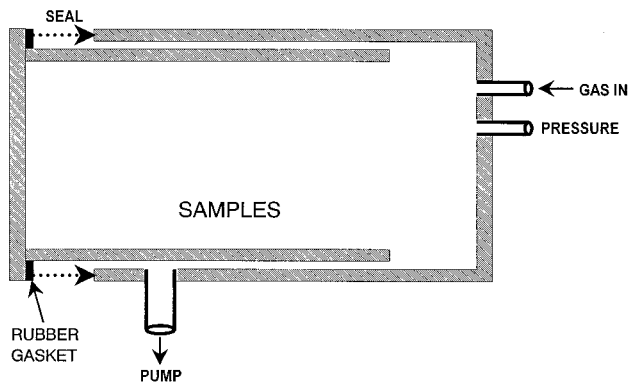


FIG. 1. Chamber design of the Plasma Prep II asher. A rubber gasket seals together two Pyrex chamber halves (shown in gray). When the two chambers are sealed, a small area of exposed rubber remains. The system base pressure is nominally 50 mT. The operating pressure of 100 mT is achieved by backfilling the chamber with oxygen. Application of 100 W rf power to electrodes surrounding the chamber creates the plasma.

in the reflectance data if contaminant films greater than about 100–200 nm were deposited during the ashing process. Also, measurable drops in specular reflectance can result from scattering or absorption of incident light by contaminant films. Fitting the reflectance data to an optical model allows quantitative measurements of film thickness when using the optical constants for SiO_2 to represent the film.

A very accurate method for determining thin film thickness and composition is variable angle spectroscopic ellipsometry (VASE[®]).^{4–6} Ellipsometric data were routinely taken at three angles of incidence over wavelengths from 250 to 1000 nm. Regression analysis was used to fit the ellipsometric parameters ψ and Δ to an optical model, permitting thickness measurements to fractions of a nanometer, making VASE ideally suited for study of thin contaminant films. Compositional information about the film can be gained through application of effective medium theory in the optical model.⁷

In addition to the optical methods described above, the composition of the contaminant layers was identified with Auger electron spectroscopy (AES).⁸ Surface coverage of the contaminant film can be studied with AES since this technique is monolayer sensitive. Acquisition of AES data while sputter etching surface layers with an ion gun yields accurate compositional depth profiles.

III. RESULTS AND DISCUSSION

A. Discovery and identification of contaminants

The first contamination study in the Plasma Prep II involved a 70-nm-thick aluminum film that had been electron-beam evaporated onto silicon. The wafer was sectioned into nine pieces and all but one were exposed in the asher. The pieces were removed one by one at 15–30 h intervals until all had been removed, resulting in nine samples with varied fluence from zero to nearly 6×10^{21} atoms/cm². Figure 2 shows the absolute specular reflectance of three of these films. Interference effects are seen with increasing exposure,

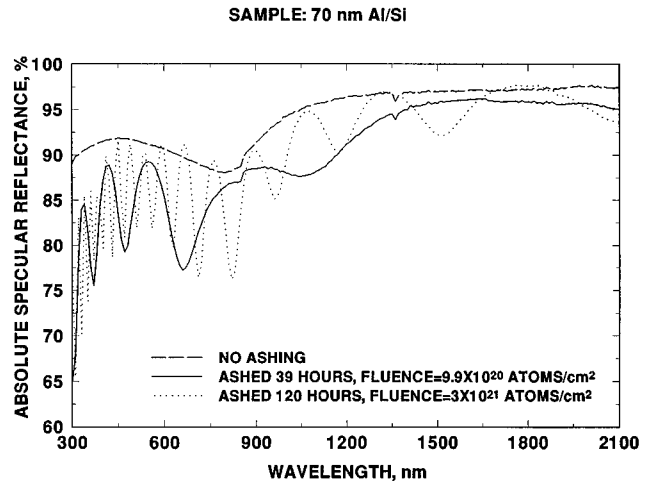


FIG. 2. Absolute specular reflectance of three identical aluminum samples. The films were electron beam evaporated onto silicon. Interference fringes appear in the data with increasing plasma exposure. An extremely thick surface film is indicated by the presence of interference fringes past 2100 nm on the film ashed to 3×10^{21} atoms/cm².

indicating the presence of a transparent film on the surface. These interference effects could be mistakenly interpreted to indicate growth of an aluminum oxide layer due to oxygen reaction. However, Fig. 2 shows pronounced interference effects at wavelengths to 2100 nm when ashed to a fluence of 3×10^{21} atoms/cm². Using a one-dimensional oxide growth model with an oxide/metal volume ratio of 1.38,⁹ the maximum possible thickness for the oxide layer would be 97 nm if all the 70 nm aluminum were converted to oxide. Using $n=1.6$ for the index of refraction of Al_2O_3 gives a quarter-wave optical thickness of 1231 nm. Figure 2 shows interference effects at a wavelength far beyond 1231 nm. This indicates that a very thick transparent layer has formed during the ashing process, and that the effects cannot be due to simple oxidation of aluminum. The decrease in specular reflectance at shorter wavelengths is attributed to scattering from roughness features formed during the ashing process. These roughness features are discussed elsewhere.¹⁰

The contaminant was identified using AES. As expected, Auger surface scans of the unashed aluminum film detect peaks due to aluminum near 1396 eV, Al_2O_3 at 51 eV, and oxygen from the native oxide layer at 503 eV.

An Auger surface scan of the film ashed 15 h to a fluence of 3.8×10^{20} atoms/cm² is shown in Fig. 3. Silicon and oxygen are seen on the surface indicating that a contaminant layer of SiO_x was deposited during ashing. The contaminant forms a continuous layer over the film since no aluminum is seen in the scan. The contaminant layer is thick compared to the Auger escape depth. The contaminant overlayer has effectively “passivated” the surface, preventing reactive species from reaching the $\text{Al}_2\text{O}_3/\text{Al}$ interface. Further evidence of this was seen in the Auger depth profile that took a total of 45 min to sputter through the oxide contaminant layer. The depth profile indicated that the value of x was very close to 2, indicating that the contaminant is nearly stoichiometric SiO_2 .

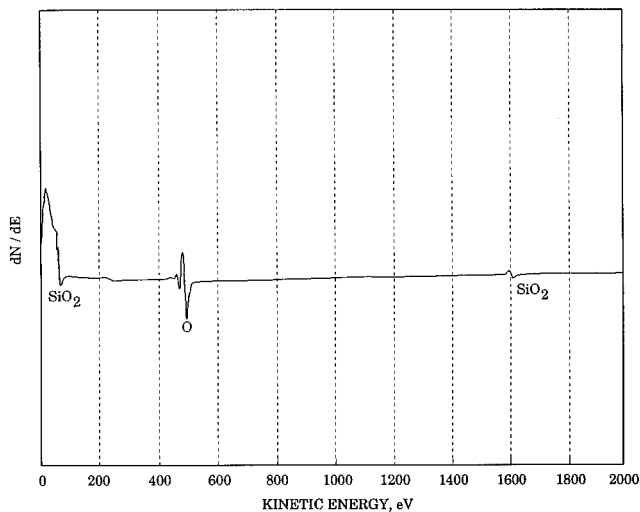


FIG. 3. Auger surface scan of an aluminum film ashed to 3.8×10^{20} atoms/cm² after 15 h of exposure. The contaminant layer has completely covered the surface in a continuous layer since no aluminum is detected. Silicon oxide (SiO_x) is easily identified as the contaminant.

The contaminant layer stoichiometry was further determined using ellipsometry. For all films used in this study the contaminant layer composition was determined, when possible, by effective medium theory to be greater than 96% SiO₂ with the remainder consisting of SiO. This is in agreement with Fig. 2 since a significant amount of optical absorption would be expected throughout the visible if a significant fraction of SiO were present. SiO is absorbing in the visible, whereas SiO₂ is transparent. Therefore, the reflectance data were satisfactorily fit using the optical constants of fully stoichiometric SiO₂ to describe the contaminant layer.

Regression analysis of the reflectance data was used to determine the thickness of the contaminant layers. The best fit optical model was found to be an aluminum film with a SiO₂ overlayer. The thin native oxide (Al₂O₃) layer was modeled as part of the SiO₂ contaminant layer since the optical data does not have independent sensitivity to both layers when one film is very thin. Parameter correlation results if the thicknesses of both layers are simultaneously fit, yielding nonunique solutions for the two layer thicknesses. Assuming the Al₂O₃ is part of the SiO₂ does not introduce significant error into the analysis because the thickness of the Al₂O₃ native oxide layer is on the order of only a few nanometers, while the SiO₂ contaminant layer thickness is hundreds to thousands of nanometers thick (the film ashed 126.5 h to a fluence of 3.2×10^{21} atoms/cm² showed a contaminant layer 1.9 μm thick). Moreover, the contaminant layer serves to quickly passivate the native oxide surface, offering further protection against oxidation of the aluminum film, and insuring that the Al₂O₃ layer remains thin during deposition of the contaminant.

The layer thickness as a function of ashing time was used to calculate the contaminant deposition rate. Fitting for contaminant layer thickness of all films as a function of asher exposure yields the deposition rate shown in Fig. 4. A con-

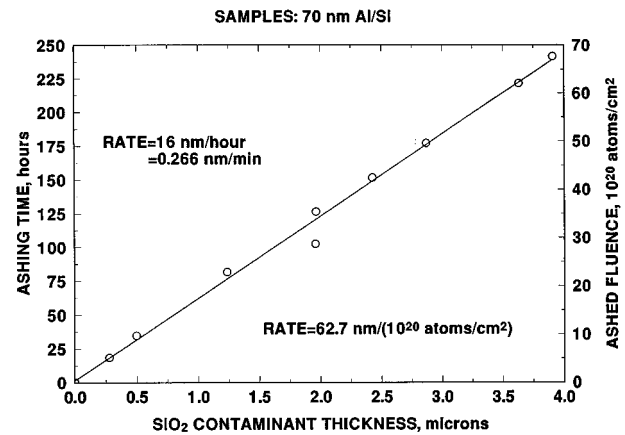


FIG. 4. Reflectance data fit for contaminant layer thickness as a function of ashing. The deposition rate was determined to be 0.27 nm/min.

stant deposition rate of 0.27 nm/min (16 nm/h) is indicated by the linear plot. Again, if the observed effects were due to oxidation of the metal film, the deposition rate would slow with exposure due to the requirement that oxygen diffuse through the oxide layer to the surface in order to continue oxidation.

Clearly, the source(s) of contaminant needed to be found. Three possible sources proved likely. First, small amounts of the silicone based pump oil could be present in the chamber through backstreaming. However, since the vapor pressure of the pump oil was approximately four orders of magnitude lower than the system operating pressure of 100 mT, this possibility seemed unlikely. This was confirmed by the addition of a molecular sieve trap to the foreline, which had no noticeable effect. A second possibility was the Pyrex chamber being etched by the plasma. This was also unlikely because the mean kinetic energy of the plasma species is on the order of 0.1 eV. Finally, the rubber gasket seal on the vacuum chamber could be etched by the plasma. Silicones present in the rubber could be broken down in the plasma and fully oxidized to SiO₂ on (or before reaching) the sample surface.

A new chamber and gasket seal were installed in order to systematically investigate contamination sources. A 100-nm-thick aluminum film sputtered onto fused silica was ashed to a fluence of 2×10^{21} atoms/cm² in a 67.25 h exposure. The contaminant layer thickness and composition were fit to the ellipsometric data. The best fit optical model was found to be a fully stoichiometric SiO₂ layer 265.3 nm thick. The raw psi and delta fit is shown in Fig. 5. The psi and delta fits are reasonably good, but a little misfit is seen between the model generated and experimental data. This is most likely due to using the refractive index of thermal SiO₂ to describe the contaminant layer. The index of thermal SiO₂ should be very close to that of the contaminant film, but it will vary slightly since the contaminant layer is not pure SiO₂, as indicated from the Auger data. Ellipsometry will be very sensitive to small changes in refractive index, but spectrophotometry will not. Therefore, the refractive index of thermal SiO₂ was used

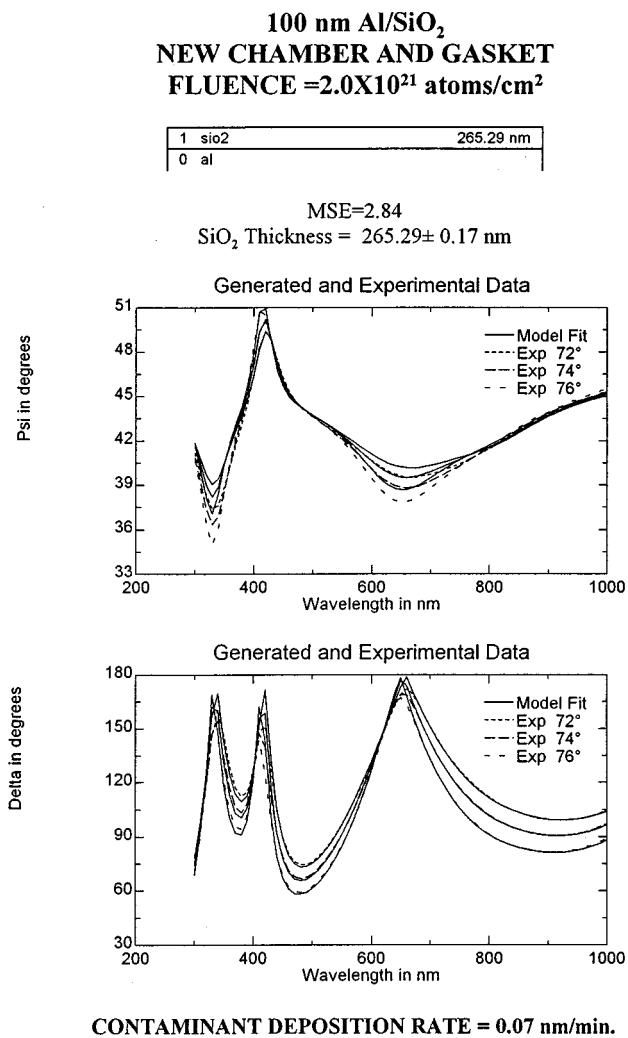


FIG. 5. Contaminant layer thickness determined by ellipsometry. A deposition rate of 0.07 nm/min was determined from film thickness of 265 nm. For this run a new Pyrex chamber and buna-n gasket were installed.

to model the contaminant layer throughout this work unless otherwise indicated.

The contaminant deposition rate was determined to be 0.07 nm/min. This is four times slower than the 0.27 nm/min determined earlier, and as expected, fewer interference fringes were present in the reflectance data.

An interesting point is that the chamber used for the initial experimental runs (shown in Fig. 2) had been used well in excess of 200 h. The buna-n gasket had dried somewhat and many small cracks were present around the exposed inside edge. This portion of the gasket was inside the vacuum and exposed to the plasma. The new gasket was unused and cracks were not present. The conclusion drawn is that contaminants are etched from the rubber gasket and settle throughout the chamber and onto the process samples. The plasma aggravates the problem by etching and oxidizing these adsorbed contaminants during exposure. In summary, it is found that etching of the gasket contaminates both the chamber and process samples.

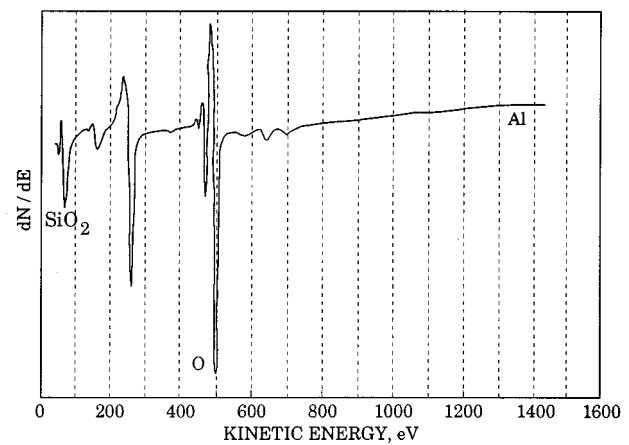


FIG. 6. Auger scan of the film ashed in the Viton sealed chamber. Chlorine and fluorine detected at 181 and 647 eV, respectively, most likely result from Viton etch products.

The chamber seal was changed from buna-n to Viton, a synthetic rubber manufactured by DuPont. Again, a 100-nm-thick sputtered aluminum film was ashed to a fluence of 2×10^{21} atoms/cm² in 67.25 h of exposure. The switch to Viton resulted in much worse contamination than with the original gasket of buna-n. The Viton gasket was visibly etched in areas where plasma exposure occurred, and a white-colored film was deposited throughout the interior of the Pyrex chamber, destroying the chamber for further ashing purposes. However, this visible etching of the gasket and subsequent contamination throughout the chamber served as further evidence of the validity of the proposed contamination mechanism, namely, plasma etching of the chamber seals results in contamination of both the chamber and samples.

An Auger surface scan of the film contaminated in the chamber sealed with Viton is shown in Fig. 6. This should be compared with Fig. 3 which shows the results obtained when the chamber was sealed with the buna-n gasket. An oxide contaminant layer has clearly covered the surface. Also, carbon is easily seen in the Auger spectra at 272 eV. The carbon most likely results from both Viton etch products as well as organic contaminants adsorbed onto the surface once vacuum was broken. Chlorine, nitrogen, and fluorine present at 181, 370, and 647 eV, respectively, may also result from Viton etch products.

This sample was characterized with ellipsometry. The best fit model was a fully stoichiometric SiO₂ layer 693.5 nm thick covering the aluminum film. The deposition rate was determined to be 0.172 nm/min. This rate is far higher than that obtained using the new buna-n gasket, but was not unexpected since the Viton gasket was etched so readily.

A method of masking the rubber gasket from direct plasma exposure was employed. A "plasma stop" was made from aluminum and fit between the two chamber halves (see Fig. 1). This plasma stop masked the exposed area of the gasket inside the chamber by fitting against the rubber seal. The metal effectively extinguished the plasma nearing the

seal by putting a good electrical conductor into its path.

Another aluminum film 100 nm thick was ashed to a fluence of 2×10^{21} atoms/cm² in 67.25 h of exposure. Reflectance data showed no interference fringes after ashing, the film appeared quite similar to unashed films (see Fig. 2). Interference fringes appear only after films have reached an optical thickness comparable to half a wavelength of the light used. Auger data showed that the surface was still covered by a continuous SiO₂ contaminant layer since no aluminum was detected.

Ellipsometry showed a contaminant film thickness of 82 nm, with a resultant deposition rate of 0.02 nm/min. This represents a factor of 13 improvement in deposition rate over the initial runs (Fig. 4). However, even this large improvement is not enough to prevent surface passivation by contaminant overlayers, indicating that the Plasma Prep II is still unsuitable for long (high fluence) ashings.

The chamber seal was once again replaced with a gasket made from urethane rubber. Direct etching of the gasket was delayed by using petroleum jelly as a vacuum grease. This was the only use of any grease with the gasket seals. Petroleum jelly, being a pure hydrocarbon, was chosen since it contains no silicones, unlike many common vacuum greases. The petroleum jelly was etched away as a sacrificial barrier to the plasma, and the hydrocarbon products were easily pumped out of the system. The petroleum jelly was applied heavily to the gasket in areas where plasma exposure would occur.

To test for contamination with this new configuration, films of both aluminum and gold were deposited onto polished wafers of silicon, gallium arsenide, and fused silica. All samples were 100 nm thick. Gold (Au) films were added since gold is extremely oxidation resistant and does not form a native oxide, making gold ideally suited for contamination studies using ellipsometry. A bulk gold layer with a SiO₂ overlayer serves as a complete optical model. This is important since the contaminant layers become thinner with improved shielding of the gasket from plasma exposure. The assumption that native oxide layers will be negligibly thin compared to the contaminant layer will no longer hold true when the contaminant layers are very thin. Thus gold allows for easy optical characterization of the contaminant.

Since it is important to show that the oxide contaminant present on the ashed films does not originate from silicon-based substrates, gallium arsenide was added as a substrate material for the films. An important result is that Auger analysis detected no gallium or arsenic at any time, indicating that the source of SiO_x contaminant is not pinholes in the metal films.

Ashing was performed in short increments on the aluminum and gold films to a total fluence of 10^{21} atoms/cm². Both specular reflectance and ellipsometric data were acquired between ashings. In the wavelength range of 300–500 nm the specular reflectance decreased with ashing as the contaminant film thickness increased.

A continuous contaminant film of SiO_x was again detected via Auger analysis, taking 12 min to depth profile

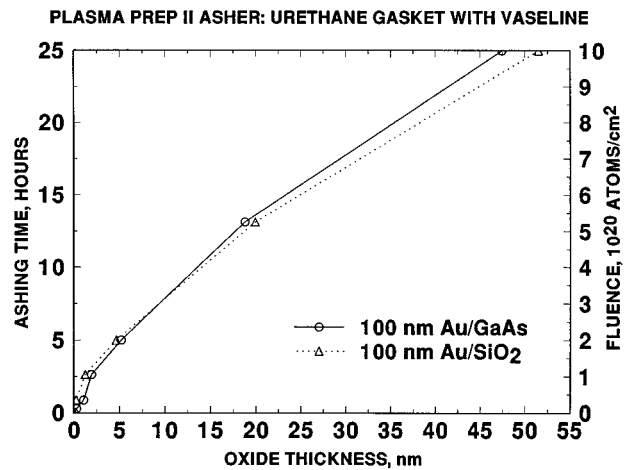


FIG. 7. Contaminant layer thickness as a function of ashing. Urethane rubber greased with petroleum jelly was used to seal the chamber. Exposure to 1×10^{21} atoms/cm² for 25 h deposits a nominal 50 nm of SiO₂ contaminant.

through the contaminant layer to reach the underlying metal film.

Ellipsometry was once again used to determine contaminant layer thickness and deposition rate. The best fit models used either a fully stoichiometric SiO₂ layer or an effective medium layer of SiO₂ and SiO to describe the contaminant film. The effective medium model fit to a SiO₂ fraction of over 96%. Ellipsometry, which is very sensitive to layer composition, shows the contaminant films to be fully stoichiometric, or nearly so. This is expected since the plasma should have plenty of time to fully oxidize adsorbed surface contaminants.

Ellipsometry was used to fit contaminant layer thickness on the gold samples as a function of plasma exposure. This is shown in Fig. 7. The SiO₂ layer thickness is nominally 50 nm for 25 h of ashing to a fluence of 10^{21} atoms/cm².

These results indicate that the level of contamination is still unacceptably high using a urethane gasket with a sacrificial barrier of petroleum jelly. The surface was still passivated by the contaminant as was indicated by Auger analysis. Although the contamination level was greatly reduced by modifying the chamber seals, it is still too high for the asher to be considered a reliable long-term space simulator.

B. Asher redesign and near elimination of contaminants

It is clear that the overall design of the chamber must be changed to confine the plasma to a volume near the process samples and well away from the chamber seals. A special-purpose chamber was designed and built at the University of Nebraska to effect the needed changes in chamber design. This redesigned chamber is shown in Fig. 8. A quartz tube is mated to a vacuum pump via a glass-to-metal seal. O-ring seals are used, but are contained within a Pyrex lip. This insures that only tiny areas of the seals would be exposed to the plasma.

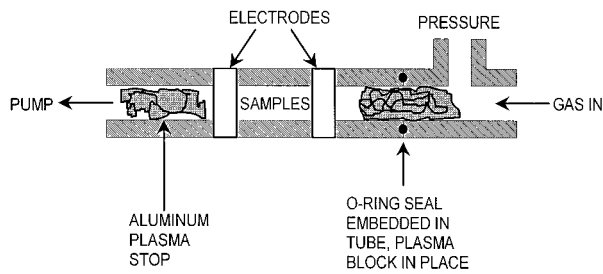


FIG. 8. Chamber design of the redesigned asher. O-ring seals embedded in a recessed Pyrex lip seal the chamber, minimizing the area exposed to the plasma. Aluminum placed into the path of the plasma effectively contains it to the processing volume. Applying 50 W rf power at 100 mT to the 5-cm-diam tube gives a flux of 1×10^{20} atoms/cm².

Since the presence of metal near the seals served to extinguish the plasma and minimize etching of the rubber, aluminum was placed inside the redesigned chamber near the seals. These plasma stops confined the plasma to a small active volume. The tube was chosen to be long enough so that the plasma stops were well away from the electrodes. This insured a uniform plasma density between the electrodes where the process samples were exposed.

The geometry of the redesigned system had the added advantage of high plasma flux. The tube diameter was approximately 5 cm. The electrode spacing was such that the flux was greater than 1×10^{20} atoms/cm²/h with 50 W applied rf power. Flux was determined through mass loss of kapton polyimide to be nearly a factor of 3 higher than that obtained running at 100 W rf power in the Plasma Prep II. The higher plasma density results from the smaller tube diameter.

The redesigned system was used to ash aluminum and gold films identical (from the same wafers) to those exposed in the Plasma Prep II with the urethane gasket. The same total fluence of 1×10^{21} atoms/cm² was repeated in exactly the same increments as before. A negligible loss in UV specular reflectance was observed on all films, indicating little change (deposited contaminant) with ashing. The same films ashed in the Plasma Prep II showed losses in UV specular reflectance with increasing plasma exposure.

Auger analysis was again used to indicate the presence of surface contaminants on films ashed in the redesigned system. An Auger surface scan is shown in Fig. 9 for an aluminum film 100 nm thick sputtered onto fused silica. This sample was ashed to a total fluence of 10^{21} atoms/cm² in 10 h of exposure. Notice the presence of Al₂O₃ at 51 and 1396 eV. Carbon and oxygen also appear at 272 and 503 eV, respectively. A small amount of SiO_x is detected at 76 eV on the ashed films and results from contamination.

These Auger results are encouraging since Al₂O₃ detected on the surface indicates that the contaminant film has not passivated the surface and is of submonolayer thickness, or nearly so, since the Auger escape depth is very small. This conclusion is supported by the ellipsometry results discussed below. The SiO₂ peak greatly receded relative to the Al₂O₃

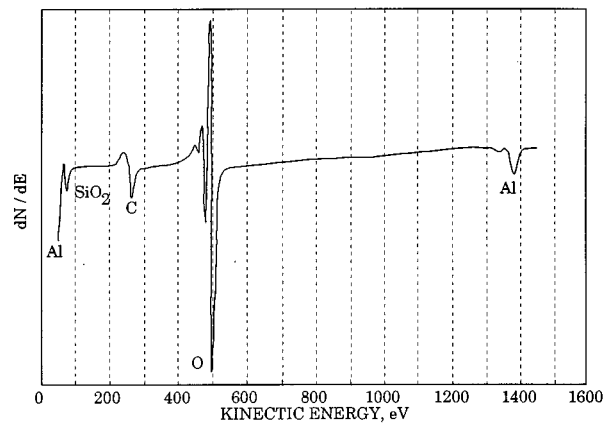


FIG. 9. Auger analysis of a 100-nm-thick aluminum film on SiO₂ ashed to 1×10^{21} atoms/cm². Aluminum oxide is still detected at 51 and 1396 eV. A small amount of SiO₂ appears at 76 eV. Some SiO₂ contamination still exists but is very minimal when compared to other samples. A continuous contaminant film has not yet formed due to the presence of Al detected in the Auger data and the absence of a surface film as determined by ellipsometry.

peak after sputtering for only 20 s with the ion gun. This indicates that a large fraction of the contaminant layer had been sputtered away in only 20 s. Elemental aluminum was detected after sputtering for 40 s indicating that the native Al₂O₃ film had also been sputtered through. No residual contaminant was detected on the film after 1 min of sputtering.

These Auger results are in contrast to those obtained in the Plasma Prep II where it took approximately 12 min to sputter through the passivating layer of 50-nm-thick SiO_x contaminant even after the chamber was sealed with the urethane gasket coated with petroleum jelly.

VASE analysis did not detect any contaminant on any films exposed in the redesigned asher. This further indicates that the small amount of contaminant detected with Auger was submonolayer in thickness. A bulk gold layer with no overcoating was the best optical model for these films. Aluminum films were modeled as a bulk aluminum layer with a thin oxide overcoat. These models are identical to those used for unashed (as-deposited) films. The Al₂O₃ layer thickness increased by only 0.2–0.3 nm during the incremental exposure to 10^{21} atoms/cm². This result, as expected, demonstrates the extreme oxidation resistance of aluminum and shows its promise as an effective space coating. Aluminum films with their native oxide layers are not much affected by oxygen plasma exposure. This result also vindicates the earlier assumption that the Al₂O₃ film thickness is negligible when compared to thick contaminant layers of SiO_x.

It is clear that the redesigned asher system deposits less than one monolayer of SiO_x contaminant even after long periods of plasma exposure. Exposures to fluences in excess of 3.5×10^{22} atoms/cm² were performed, with Auger data still showing less than one monolayer of contaminant. This fluence is equal to 7.5 years of orbital exposure expected on the International Space Station. From the Auger data it ap-

TABLE I. Summary of the methods used to reduce contamination in oxygen plasma ashers. Aluminum placed near the rubber seals greatly reduces contamination.

Asher configuration	Contaminant deposition rate (nm/min)	Contaminant deposition rate nm/(10 ²¹ /atoms/cm ²)	Comments
Used chamber, buna-N gasket	0.27	62.7	Chamber used for ~200 h
New chamber, new buna-N gasket	0.07	13.3	Chamber not used before
New chamber, Viton gasket	0.17	34.7	Do not use! Viton etches and deposits onto chamber!
New chamber, new buna-N gasket, Al ring plasma stop	0.02	4.1	Chamber not used before
New chamber, urethane gasket, petroleum jelly grease barrier	0.09	5.2	Petroleum jelly serves as a sacrificial hydrocarbon barrier
Quartz tube asher, custom design plasma stopped before gasket reached	Submonolayer	Submonolayer	AES shows submonolayer of contaminant for fluence=3.5×10 ²² atoms/cm ² no optical changes seen

pears that much longer ashings to higher fluences are possible in the redesigned system without surface passivation from contaminant layers.

Table I summarizes all the methods used to minimize contamination and their effectiveness.

IV. CONCLUSIONS

Quantitative evaluation of materials for use in low Earth orbit is severely hampered by contamination inside plasma ashing chambers. Etching of rubber chamber seals serves as a major source of SiO_x contaminants. Contaminant deposition rates reached 0.27 nm/min in the worst case. Even after short exposures, contaminants can passivate the surface of interest, destroying the chances for accurate simulation of space degradation.

The commercially available Plasma Prep II system is poorly designed against contamination due to a chamber geometry that allows etching of the rubber gasket seal, but steps can be taken to considerably lower the level of contamination using this system. A redesigned system confines the plasma to the processing volume only and has proven far more effective in reducing contamination. Using the redesigned system, less than a single monolayer of contaminant was deposited for fluences greater than 3.5×10²² atoms/cm².

ACKNOWLEDGMENTS

Dr. John Pouch of the NASA-Lewis Research Center deserves a special thank you from the authors for contributing part of the Auger data presented here. Useful discussions were also held with members of Bruce Banks group at the NASA-Lewis Research Center. This research was supported by NASA-Lewis Research Center Grant No. NAG-3-95.

¹D. A. Gulino, in *Surface Modification Technologies II*, edited by T. S. Sudarshan and D. G. Bhat (The Minerals Metals and Materials Society, 1989), pp. 73–90.

²K. K. DeGroh, J. A. Terlep, and T. M. Dever, 5th Annual Air Force Workshop on Surface Reactions in the Space Environment, Evanston, IL, September 1990 (unpublished).

³S. K. Rutledge *et al.*, NASA Technical memo, No. 100122, 1986.

⁴J. A. Woollam and P. G. Snyder, *Mater. Sci. Eng. B* **5**, 279 (1990).

⁵S. A. Alterovitz, J. A. Woollam, and P. G. Snyder, *Solid State Technol.* **31**, 99 (1988).

⁶R. M. A. Azzam and N. M. Bashara, *Ellipsometry and Polarized Light* (North-Holland, New York, 1977).

⁷D. E. Aspnes, J. B. Theeten, and F. Hottier, *Phys. Rev. B* **20**, 3292 (1979).

⁸L. C. Feldman and J. W. Mayer, *Fundamentals of Surface and Thin Film Analysis* (North-Holland, New York, 1986).

⁹W. F. Smith, *Principles of Materials Science and Engineering* (McGraw-Hill, New York, 1990).

¹⁰R. A. Synowicki, R. D. Kubik, J. S. Hale, J. Peterkin, S. Nafis, J. A. Woollam, and S. Zaat, *Thin Solid Films* **206**, 254 (1991).